CrossMark

Merits and Demerits of Transparent Conducting Magnetron Sputtered ZnO:Al, ITO and SnO$_2$:F Thin Films for Solar Cell Applications

Rajesh Das[1] · Himadri Sekhar Das[1]

Abstract Transparent conducting ZnO:Al and indium tin oxide (ITO) thin films were deposited by magnetron sputtering under reactive environment. Both the transparent conducting oxide (TCO) films were exposed intentionally in hydrogen environment at 350 °C calcinations temperature to study the post treated TCO film's opto-electronic, structural as well as surface morphological properties. Electrical resistivity of both ZnO:Al, ITO and SnO$_2$:F films are comparable (order of 10^{-4} Ω-cm), lowest sheet resistance are 8.5, 3.7 and 4.6 Ω/sq respectively and slightly improved after hydrogen exposure at 350 °C. Optical transmittance and internal texture of hydrogen environment exposed ZnO films remains invariant, but in case of ITO, SnO$_2$:F films optical transmittance deteriorated drastically. Hexagonal wurtzite structure with (002) c-axis orientation is observed for pre- and post-hydrogen exposed ZnO films whereas internal texture as well as crystallographic orientation of ITO and SnO$_2$:F films have significantly changed. Surface grains of ITO films have been significantly enhanced, but no such variations are observed in ZnO surface morphology. ZnO:Al and ITO films show unique plasmonic properties in near infrared transmittance due to free carrier generation in conduction band. Based on surface features/morphology, haze factor and internal texture light scattering mechanism is modeled.

Introduction

Transparent conductive oxide (TCO) films are most important material from technological point of view mainly for its wide applications in various electronic and opto-electronic devices, such as solar cells, gas sensors, varistors, organic material based microelectronic, polymer electronics and diodes due to their unique materials properties such as high electrical conductivity and high optical transmittance [1–5]. Among them magnetron sputtered fluorine doped tin oxide (SnO$_2$:F), indium tin oxide (ITO), and aluminum doped zinc oxide (ZnO:Al) thin films are most attractive materials for their non-toxicity, ease of availability, high sticking co-efficient with substrate materials and unique opto-electronic properties.

TCO thin films with unique low sheet resistance (<10 Ω/sq), almost 90 % optical transmission, its wide band gap ($E_g \sim 3.9$ eV) and high refractive index ($\mu \sim 2$) acts as window layer to visible and near infra-red (NIR) region of solar spectrum. ITO can form rectifying contact as plasmonic metamaterial and ohmic contact with shallow emitter layer [6].

Parida et al. [4] fabricated Si-based p–i–n solar cell using thin layer of ITO films as buffer layer and reported IR induced ITO plasmon excitation and conduction electron excitation. DuBow et al. [6] fabricated efficient thin film solar cell using ITO thin film, that forms ohmic contact on n-Si and rectifying contact on p-Si, and hence enhances short circuit current density (J_{sc}). Increase in short circuit current is due to carrier excitation behavior at conduction band for the IR spectra induced plasmonic

✉ Rajesh Das
rajesh_eru2003@yahoo.com

1 Haldia Institute of Technology, Haldia, Purba Medinipur 721 657, West Bengal, India

86

J. Inst. Eng. India Ser. D (January–June 2017) 98(1):85–90

metamaterial effect of metallic ITO thin film. IR absorption causes carrier excitation and carrier formation within the conduction band that indicates the metallic nature of ITO films on the functions of plasmons and blocks the incident light as a metal like mirror [4]. ZnO:Al is very much suitable for micro-crystalline based Si-thin film solar cell fabrication, where high hydrogen dilution is incorporated with silane (SiH_4) precursor gas [7]. Hydrogen acts as reducing agent for transparent conducting oxide (TCO) thin film. But ZnO is more stable under hydrogen plasma environment, ITO and SnO_2:F degrades very quickly under hydrogen plasma.

RF-sputtered ITO films with all suitable electrical and optical properties can produce high IR-reflecting properties due to its high carrier concentration. As grown ITO thin films are usually non-stoichiometric due to their large number of oxygen vacancies as well as substitutional Sn dopants and it becomes degenerate n-type semiconductors [8–10]. Metallic behaviour and plasmonic metamaterial effect in TCO films can be enhanced by high temperature hydrogen exposure with increase of carrier concentration.

In this study, we have investigated different merits and demerits of different TCO thin films in context of thin film solar cell applications. Role of H_2 dilution in controlling internal textures, establishment of plasmonic behavior as well as morphological changes with the variation of elemental composition are discussed. Effect of post hydrogen plasma treatment on electrical, optical, structural and morphological properties of ITO films is also reported. Based on the change of surface morphology, internal texture and optical properties, the optical model is introduced.

Experimental

ZnO:Al and ITO thin films are prepared by dual-target RF magnetron sputtering system on glass substrate at substrate temperature $T_s = 300\ °C$ using 99.99 % pure sintered ceramic disc of ZnO:Al (2 wt % Al), ITO [indium oxide (90 %) and tin oxide (10 %) by weight] sputtering target by Ar, Ar + O_2 and Ar + H_2 as sputtering gas. The electrical resistivity, carrier density and Hall mobility of ITO thin films were studied by 4-probe van-der-Pauw technique attached with Hall measurement (Ecopia-HMS-3000) set-up. Optical transmittance and absorbance data of ZnO thin films were measured using microprocessor controlled dual beam UV–VIS spectrophotometer (Perkin-Elmer Lamda-35). Structural characterization of TCO films was carried out by Crystallographic phase analysis X-ray diffraction (XRD) (Philips PW 1710 diffractometer) (Cu K_α, $\lambda = 1.54178$ Å, 2θ scan mode). The surface morphology was performed by Scanning Electron Microscopy (SEM) (Carl Zeiss SMT Supra 55). Elemental analysis was estimated by Energy dispersive X-ray spectroscopy (EDX) attached with SEM.

Results and Discussion

ZnO thin films were deposited with 80 W RF-power, 10 mbar chamber pressure, 300 °C substrate temperature with controlled substrate rotation under reactive environment. ZnO:Al films show promising electrical properties ($\rho = 3.89 \times 10^{-4}$ Ω-cm and $R_{sh} = 7.65$ Ω/sq) due to its high carrier density and almost 90 % optical transmission. Those properties are comparable with sputtered ITO and U-type SnO_2:F thin films ($R_{sh} < 5$ Ω/sq) due to both high carrier density ($\sim 10^{20}/cm^{-3}$) and mobility. Temperature dependent electrical resistivity, carrier concentration and mobility of as deposited ZnO:Al films (up to substrate temperature $T_s = 400\ °C$) deposited under hydrogen environment is shown in Table 1. It was observed that resistivity decreases as the deposition temperature increases up to 300 °C, but above 300 °C the resistivity increases due to increases of free carrier scattering, grain boundary scattering and for lowering of mobility. Important observations are made for atomic hydrogen exposed TCO films. The details of the results, electrical properties and optical properties are shown below in Table 2.

In presence of high atomic hydrogen exposure (40 sccm) at 350 °C calcinations temperature the electrical resistivity and optical transmission remains unaltered but for ITO and SnO_2:F films the same are drastically deteriorated (shown in Fig. 1).

Under excessive H_2 dilution oxygen deficient zinc-blende phase are formed instead of wurtzite structure. O-deficient or Zn rich films are formed, Zn^{2+} ion will be replaced by Al^{3+} ions or Zn-H bond can be formed that contributes in enhancement of free carrier density without disturbance of optical transmission [1, 11]. But for ITO and SnO_2:F thin films more metallic nature is created, so electrical sheet resistance and optical transmission drastically deteriorated due to low binding energy.

Figure 1 shows the optical transmittance spectra of as deposited and hydrogen treated ZnO, ITO and SnO_2:F

Table 1 Variation of electrical parameter

Substrate temperature T_s (°C)	Resistivity (Ω-cm)	Mobility (cm^2/V s)	Carrier concentration/cm^3
200	8.6×10^{-3}	1.2	5.7×10^{20}
250	6.2×10^{-4}	3.1	3.2×10^{21}
300	3.89×10^{-4}	4	4.1×10^{21}
350	4.8×10^{-4}	3	4.3×10^{21}
400	5.7×10^{-3}	0.25	4.3×10^{21}

Table 2 Comparative results of electrical and optical properties

Sample (ITO) C_H values	Carrier concentration (cm^{-3})	Mobility (μ) (cm^2/V s)	Resistivity (ρ) (Ω-cm)	% Optical transmittance (T) @ 500 nm	Sheet resistance $R_{sh} = (\rho/t)$ Ω/sq	Figure of merit $\phi^{TC} = T^{10}/R_{sh}$
SnO$_2$:F	7.35×10^{20}	18.37	2.78×10^{-4}	87	4.63	1.50×10^{19}
Atomic hydrogen exposed SnO$_2$:F	7.35×10^{20}	8.37	2.78×10^{-3}	32	4.13	2.70×10^{14}
As deposited ITO	1.73×10^{21}	11.58	3.12×10^{-4}	85	5.2	6.70×10^{18}
Atomic Hydrogen exposed	5.89×10^{21}	1.10	4.37×10^{-3}	57	12.35	2.9×10^{16}
As deposited ZnO	1.80×10^{21}	8.93	3.89×10^{-4}	91.2	7.65	4.76×10^{18}
Atomic hydrogen exposed ZnO:Al	3.27×10^{21}	9.25	3.54×10^{-4}	90.2	6.75	5.1×10^{18}

films; significant deterioration in visible optical transmission is observed for ITO and SnO$_2$:F films. In the experimental arrangement 40 sccm H$_2$ gas was passed at 350 °C substrate temperature for 2 min. Optical transmittance of ITO films becomes less than 60 % at 500–700 nm range. In case of SnO$_2$:F visible optical transmission falls drastically from 85 to 35 % in overall solar spectrum but ZnO:Al films remains un-deteriorated.

Hexagonal wurtzite (002) orientations are observed for both as deposited and hydrogen treated ZnO:Al film (not shown here). Intensity of (002) preferred orientation of ZnO:Al films decreases, that causes the reduction of grain size. Figure 2a shows the X-ray diffraction patterns of as deposited and hydrogen exposed ITO films, peaks were indexed according to the ASTM powder data. The texture coefficient TC (hkl) have been calculated from the X-ray data using the well-known formula [12] given by

$$TC(hkl) = \frac{I(hkl)/I_o(hkl)}{N^{-1}\sum_n I(hkl)/I_o(hkl)} \quad (1)$$

where I(hkl) is the measured relative intensity of a plane (hkl), I$_o$(hkl) is the standard intensity of the plane (hkl) taken from the JCPDS data, N is the reflection number and n is the number of diffraction peaks. TC (hkl) values for major three peaks of the thin films are presented.

In Fig. 2a, curve-1, represents highly polycrystalline ITO films with (211), (222), (400), (111), (024), (044), (611) and (622) crystalline planes of In$_2$O$_3$. In curve-1, the relatively high intensity of two preferred orientations (222) and (400) planes refers the parallel to the substrate, sharp (222) phase refers cubic bixbyite structure of In$_2$O$_3$. The less intensity small broad peaks (211), (111), (024), (044), (611) and (622) refers to crystallographic defects and amorphization processes in the large In$_2$O$_3$ and SnO$_2$ grains. The nature of the created defects in In$_2$O$_3$ and SnO$_2$ crystallites are identical due to nearly identical masses of indium and tin. Curve-2 represents the drastically intensified (400) X-ray diffraction peak of

atomic hydrogen exposed ITO film at 350 °C. Intense (400) peak means deterioration of film's compactness and increases of number of inter grain voids/defects.

The ratio of texture co-efficient of as deposited to hydrogen exposed ITO film becomes 2:3 and 6:1 for (400) and (222) peaks respectively. That indicates improved crystallinity along (400) direction. Atomic hydrogen creates more oxygen vacancies in ITO matrix and aggregation of SnO$_2$ and SnO phases, that substitute's indium in the BCC lattice creates bigger surface grains (shown in SEM micrograph of degraded ITO films). Increase of metallic components increase the carrier density in ITO films and plasmonic behavior becomes more prominent in hydrogen treated ITO films.

Figure 2b shows the as deposited and atomic hydrogen exposed SnO$_2$:F films. Curve-1, represents highly polycrystalline SnO$_2$:F films with intense (110) and (111) peaks and other less intense peaks (101), (211), (220), (310) and (301) respectively before atomic hydrogen exposure. Curve-2 shows the X-ray diffraction spectrum of atomic hydrogen exposed SnO$_2$:F film at 350 °C calcinations temperature with (200), (102) and (112) orientations. Here some new intense SnO$_2$ peaks with variable texture co-efficient are observed. From the XRD analysis it is observed that few XRD peaks of ITO and SnO$_2$:F films are intensified drastically and FWHM (Full Width Half Maximum) decreases, therefore the grain size becomes larger in case of hydrogen exposed ITO films. In some cases of SnO$_2$:F films peaks FWHM increases and hence grain size decreases.

Effect of Surface Texture

Surface texture is achieved generally by wet Chemical Etching as well as plasma etching. With increase of etching, Surface roughness increases and Haze factor also increases. With increase of surface roughness specular transmission decreases and diffuse scattering predominates.
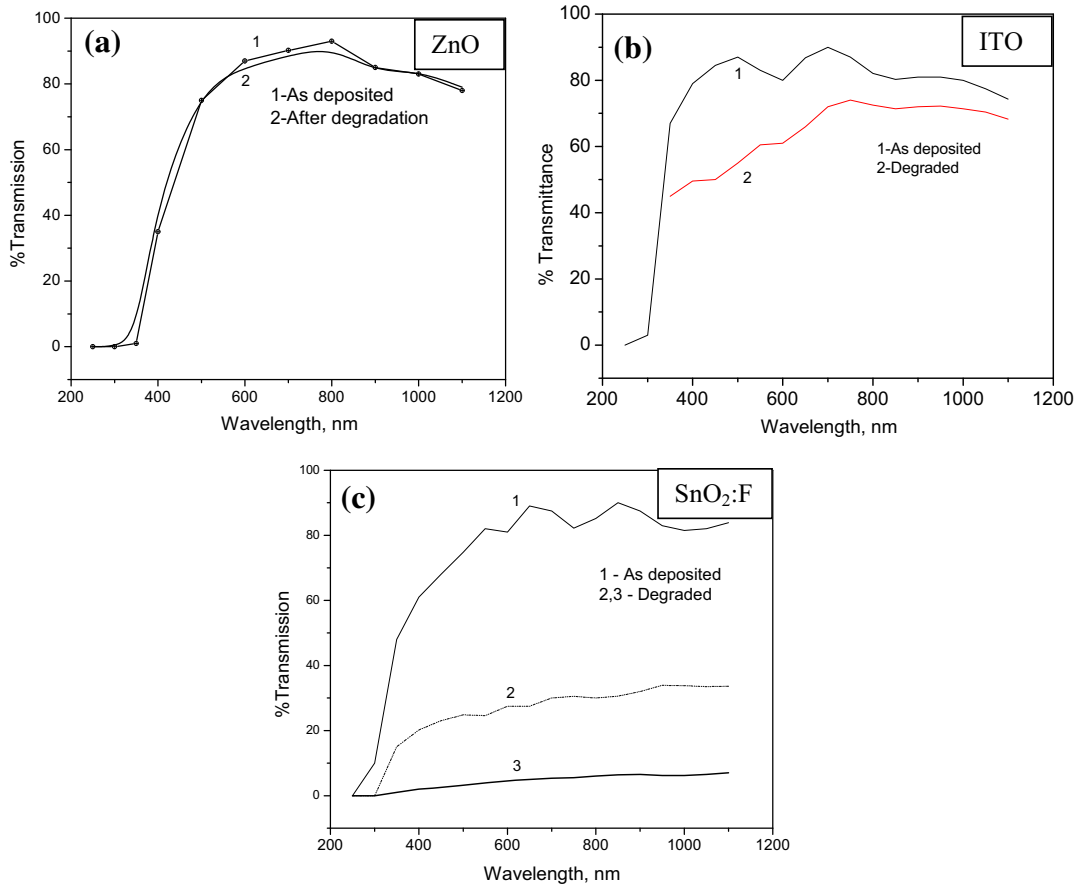
88

J. Inst. Eng. India Ser. D (January–June 2017) 98(1):85–90

Fig. 1 Optical transmittance (*1* before and *2,3* after H-plasma exposure) of RF-sputtered **a** ZnO:Al film, **b** ITO film and **c** SnO$_2$:F film
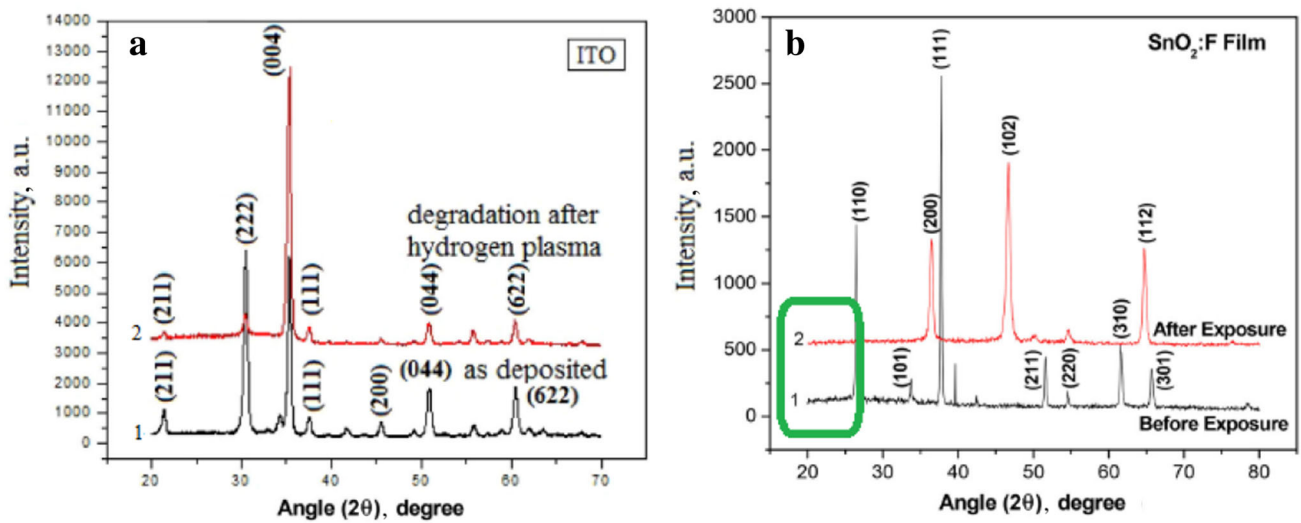

Fig. 2 X-ray diffraction spectra of **a** ITO and **b** SnO$_2$:F films. *Curve-1*: before H-plasma exposure and *Curve-2*: after hydrogen plasma exposed

The total reflection of light from a surface of normally distributed height is given by

$$R_F = R_0 \exp\left[\frac{(-4\pi\sigma)}{\lambda^2}\right] + \left(\frac{32R_0}{m^2}\right)\left(\frac{\pi\sigma}{\lambda}\right)^4 (\Delta\theta)^2 \quad (2)$$

where, λ wavelength, σ RMS roughness, m mean gradient of the surface, R_0 reflectivity of the coating, $\Delta\theta$ solid angle of the measurement.

In the above expression the 1st term corresponds to specular scattering and 2nd term corresponds the diffuse

Fig. 3 Scanning electron micrograph of **1**, **2** ITO thin film (**1** before and **2** hydrogen exposed), **3**, **4** SnO₂:F thin film (**3** before and **4** hydrogen exposed) and **b** ZnO:Al film (hydrogen exposed)
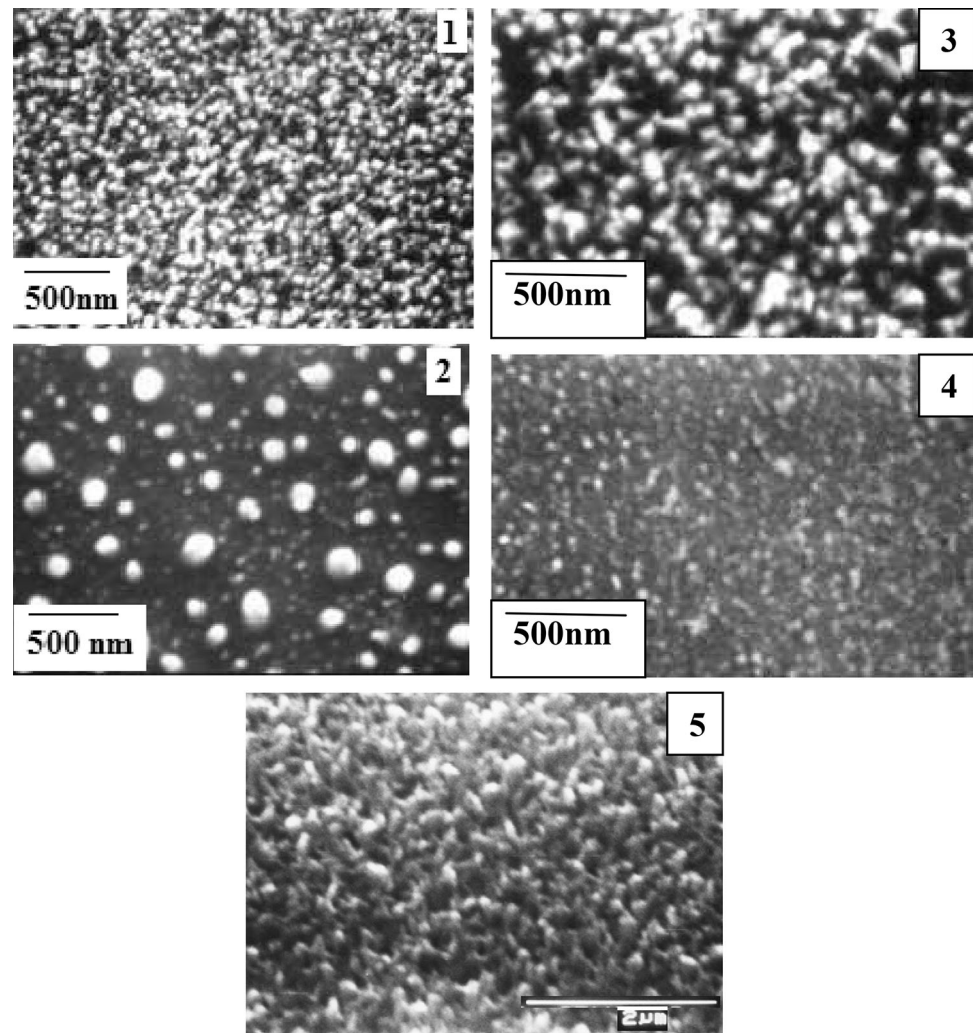
scattering. When the surface roughness (σ) increases, diffuse scattering predominates.

As deposited ZnO:Al films under various hydrogen dilution ratio shows different haze factor and ultimately affects light scattering mechanism. The haze factor was defined as the ratio of diffused transmittance with total transmittance. Before hydrogen exposure the ZnO:Al thin film surface is smooth, but after hydrogen exposure the surface becomes more textured shown in SEM image in Fig. 3 [5]. These surface texturization further increases rough surfaces that will increase the diffused light scattering from the surface. In case of heat treated ZnO:Al thin films under H_2 environment, haze factor increases from 32.5 to 35 %. For ZnO:Al film with mostly flat surface, both the specular and partial diffuse scattering mechanism exist. However, for ZnO:Al film with very rough surface, the diffuse scattering predominates which is inelastic or random. During post deposited hydrogen exposure at 350 °C, ZnO:Al film surface profile may be changed due to reduction of oxygen atom from lattice site

and hence improves effective surface roughness scattering.

In case of hydrogen exposed ITO thin film at 350 °C surface morphology drastically deteriorated. Grain sized becomes around 500 nm, surface roughness profile is changed (Surface morphology shown in SEM image). But optical transmission has been drastically deteriorated.

Figure 3 (3, 4) shows the as deposited and hydrogen exposed SnO₂:F thin films where nano surface grains are formed after atomic hydrogen exposed SnO₂:F films.

In thin film solar cell applications, TCO material is used to provide a window for the incident illumination to the device and also serves as one of the electrodes of solar cell. The ideal TCO provides high transparency over a wide spectral range with high conductivity and higher carrier mobility. Textured TCO provides light scattering, which increases the optical absorption of weakly absorbed light in the solar cells.

The generation term is calculated via an Optical Model where both specular interferential effects and diffuse

90

J. Inst. Eng. India Ser. D (January–June 2017) 98(1):85–90
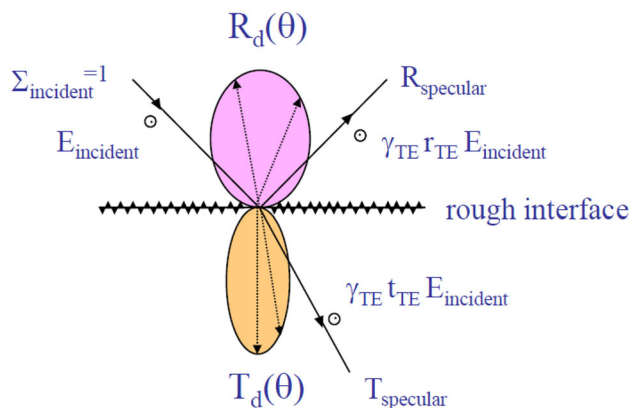
Fig. 4 Schematic illustration of optical model for the specular and diffuse transmission and reflection at rough TCO and a-Si/μc-Si thin film interface
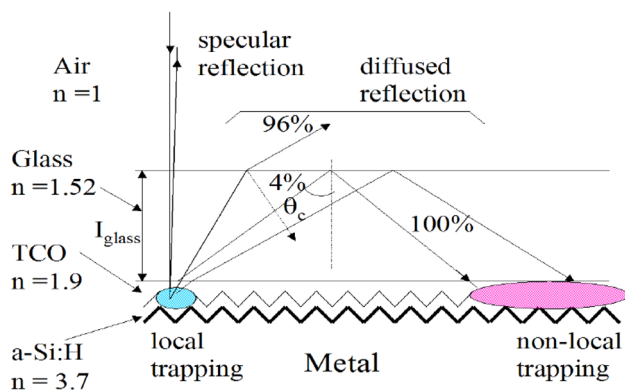
Fig. 5 Schematic diagram of light trapping in p–i–n solar cell: local and non-local light trapping

reflectances and transmittances due to interface roughness should be taken into account. The light scattering mechanism and light trapping are shown in the Figs. 4 and 5 respectively.

Details of scattering model for TCO coated substrate are discussed and reported and have been found to be in good agreement with experimental value with the theoretical prediction based on moderate surface roughness [surface roughness (δ_{rms}) $\sim$ 40 nm for SnO$_2$ thin film and 50 nm for ZnO:Al thin film] by Jäger and Zeman [13].

Conclusions

Details of electrical, optical, structural and morphological properties of different TCO films are discussed in detail. ZnO:Al films are highly resistant in hydrogen exposure at 350 °C calcinations temperature. Internal texture remains unaltered along c-axis orientation with (002) crystallographic direction. Surface texture is modified due to oxygen reduction from its lattice site under high temperature hydrogen exposure. Surface modification can play more significant role to achieve enhanced and stable solar cell fabrication. ITO and SnO$_2$:F are less stable in hydrogen environment due to low binding energy and optical properties drastically falls. ITO and SnO$_2$:F films are not suitable for thin micro-crystalline Si-solar cell fabrication. But, plasmonic meta-material and metallic behavior may be helpful for application as counter electrode in dye-sensitized solar cell to replace Pt-coated TCO film. Hydrogen exposure can tune the surface texture, and based on surface profile optical model of light scattering has been modeled and light trapping mechanism also are predicted.

References

1. R. Das, K. Adhikary, S. Ray, Jpn. J. Appl. Phys. **47**, 1501 (2008)
2. W.J. Jeong, S.K. Kim, G.C. Park, Thin Solid Films **506–507**, 180 (2006)
3. S.Y. Lien, Thin Solid Films **518**, S10 (2010)
4. B. Parida, H.Y. Ji, G.H. Lim, S. Park, K. Kim, J. Renew. Sustain. Energy **6**, 053120 (2014)
5. E. Gur, S. Tuzemen, B. Kilic, C. Coskun, J. Phys. Condens. Matter. **19**, 196206 (2007)
6. J.B. DuBow, D.E. Burkt, J.R. Sites, Appl. Phys. Lett. **29**, 494 (1976)
7. Bannerjee, et al. J. Phys. D Appl. Phys. **26**, 2144–2147 (1993)
8. M. Nisha, S. Anusha, A. Antony, R. Manoj, M.K. Jayaraj, Appl. Surf. Sci. **252**, 1430 (2005)
9. F.E. Akkad, M. Marafi, A. Punnoose, G. Prabu, Phys. Status Solidi **177**, 445 (2000)
10. W. Wohlmuth, I. Adesida, Thin Solid Films **479**, 223 (2005)
11. W.W. Wang, X.G. Diao, Z. Wang, M. Yang, Z. Wub, Thin Solid Films **491**, 54 (2005)
12. Y. Caglar, M. Zor, N. Caglar, S. Ilican, J. Optoelectron. Adv. Mater. **8**(5), 1867 (2006)
13. K. Jäger, M. Zeman, Appl. Phys. Lett. **95**, 171108 (2009)